Alkalinity sources in the Dutch Wadden Sea

Mona Norbisrath[1,2,3], Justus E. E. van Beusekom[1], & Helmuth Thomas[1,2]

[1]Institute of Carbon Cycles, Helmholtz-Zentrum Hereon, Geesthacht, 21502, Germany

[2]Institute for Chemistry and Biology of the Marine Environment (ICBM), Carl von Ossietzky University Oldenburg, Oldenburg, 26129, Germany

[3]now at: Department of Marine Chemistry and Geochemistry, Woods Hole Oceanographic Institution, Woods Hole, MA, 02543, USA

Correspondence to: Mona Norbisrath (mona.norbisrath@whoi.edu)

Abstract

The oceanic buffering capacity total alkalinity (TA), as the major global CO_2 sink, is of growing scientific interest. TA is mainly generated by weathering, and further by various anaerobic metabolic processes. The Wadden Sea, located in the southern North Sea is hypothesized to be a source of TA for the North Sea, but quantifications are scarce. This study observed TA, dissolved inorganic carbon (DIC), and nutrients in the Dutch Wadden Sea in May 2019. Along several transects, surface samples were taken to investigate spatial distribution patterns and to compare them with data from the late 1980s. A tidal cycle was sampled to further shed light on TA generation and potential TA sources. We identified the Wadden Sea as a source of TA with an average TA generation of 7.6 µmol kg^{-1} h^{-1} TA during ebb tide in the Ameland Inlet. TA was generated in the sediments with deep pore water flow during low tide enriching the surface water. A combination of anaerobic processes and $CaCO_3$ dissolution were potential sources of TA in the sediments. We assume that seasonality and the associated nitrate availability in particular influence TA generation by denitrification, which we assume is low in spring and summer.

1 Introduction

As the regulator of the ocean carbon dioxide (CO_2) sink, total alkalinity (TA) is of increasing scientific interest and is investigated worldwide in the Anthropocene (Abril and Frankignoulle, 2001;Bozec et al., 2005;Chen and Wang, 1999;Dickson, 1981;Middelburg et al., 2020;Norbisrath et al., 2022;Renforth and Henderson, 2017;Thomas et al., 2004;2009;Sabine et al., 2004). The Anthropocene describes the current era of our planet, when environmental changes, driven by humans, have become identifiable in geological records (Zalasiewicz et al., 2010;Crutzen, 2002). The climate and the increasing atmospheric CO_2 content is mainly regulated by the open ocean. Around 30 % of the global anthropogenic CO_2 emissions are removed by the ocean (Gruber et al., 2019). The carbon storage capacity of the North Sea is an important atmospheric CO_2 sink as it exports the absorbed CO_2 in the deep layers of the Atlantic Ocean where it is stored on longer time scales (Borges et al., 2005;Bozec et al., 2005;Burt et al., 2016;Brenner et al., 2016;Hu and Cai, 2011;Schwichtenberg et al.,

2020;Thomas et al., 2004;2009). Two important aspects of the oceanic climate regulation are the oceanic circulation and TA. Both interact well in highly active and shallow ocean areas such coastal zones and continental and marginal shelves. In these shallow areas, TA is very susceptible due to various metabolic processes and the influence of adjacent zones like rivers, estuaries, marshes, and tidal flats (e.g., Norbisrath et al., 2022;2023;Wang et al., 2016;Voynova et al., 2019). A previous study by Norbisrath et al. (2022) showed that an enhanced riverine, metabolic alkalinity would lead to increasing CO_2 absorption in the coastal zones of the North Sea, highlighting the need to further investigate TA regulation in adjacent zones of coastal oceans.

Coastal zones, which are the direct interface between most, if not all, compartments of the Earth system (i.e., terrestrial, aquatic, oceanic) and human societies, appear particularly vulnerable to environmental and climate change (Glavovic et al., 2015). This holds true for the Wadden Sea, the shallow, coastal sea along an approximately 500 km coastline of the Netherlands, Germany, and Denmark, in the southern North Sea, which is declared as an UNESCO world natural heritage site since 2009. Most of the Wadden Sea is located between the protecting barrier Islands and the Mainland, which makes it the world's largest uninterrupted stretch of tidal flats with multiple tidal inlets (Fig. 1). Due to the topography, the Wadden Sea is a highly dynamic ecosystem with influences from the mainland and the North Sea (Hoppema, 1993;Postma, 1954;van Raaphorst and van der Veer, 1990). Driving forces of the biogeochemical dynamics in the Wadden Sea are nutrient and organic matter (OM) imports by rivers and high suspended particulate matter (SPM) imports from the North Sea (Van Beusekom et al., 2012;Postma, 1954). Physical sources of variability in the Wadden Sea are oceanic driven wind, waves, and tidal currents, as well as the counterclockwise circulation of the North Sea (Elias et al., 2012). Large tidal amplitude and currents in conjunction with shallow water depths allow for vertical water column mixing and an exchange between the pelagic and benthic realms including deep pore water exchange (Røy et al., 2008). The high tidal currents also impact the biogeochemistry of the North Sea (Postma, 1954), as they cause an exchange of water between the North Sea and the Wadden Sea and play an important role in the import of particulate matter from the North Sea (Burchard et al., 2008).

TA, primarily consisting of bicarbonate and carbonate, is generated by chemical rock weathering (Suchet and Probst, 1993;Meybeck, 1987;Berner et al., 1983), and in various stoichiometries by calcium carbonate ($CaCO_3$) dissolution and anaerobic metabolic processes, such as denitrification, which is the reduction process of nitrate to dinitrogen gas in the nitrogen cycle (Hu and Cai, 2011;Wolf-Gladrow et al., 2007;Chen and Wang, 1999;Brewer and Goldman, 1976). Understanding of TA sources have recently become increasingly important due to increasing anthropogenic CO_2 emissions, and the resulting demand for ocean based net-negative CO_2 emissions (e.g., Keith et al., 2006;Matthews and Caldeira, 2008;Zhang et al., 2022). In previous studies, the Wadden Sea was identified as a TA source for the North Sea with a loading between 39 Gmol yr^{-1} (Schwichtenberg et al., 2020) and 73 Gmol yr^{-1} (Thomas et al., 2009). Both studies suggested the entire Wadden Sea as one of the most important TA sources of the carbon storage capacity for the North Sea. Burt et al. (2016) highlighted the importance of coastal TA production for regulating the buffer system in the North Sea, and suggested denitrification as the major TA source. Due to the strong connection between the North Sea and the Wadden Sea, a better understanding of TA generation in the latter is required. Here, we focus on the Dutch Wadden Sea that has been well-studied during the past decades (Hoppema,

1990, 1991, 1993;De Jonge et al., 1993;Elias et al., 2012;Ridderinkhof et al., 1990;Postma, 1954;Van Beusekom et al., 2019;Schwichtenberg et al., 2017). In particular Hoppema (1990);(1993) observed the spatial and temporal variability of TA in May, which we compare with our observed transect data to detect potential differences over the last 30 years. In addition, we further shed light on potential TA sources in the Dutch Wadden Sea.

2 Methods

2.1 Study site and sampling

This study is based on samples collected on a research cruise (LP20190515) in the Dutch Wadden Sea (Frisian Islands) on RV *Ludwig Prandtl* in May 2019 (Fig. 1). We collected water samples in the Wadden Sea starting at Harlingen, through the Vlie Inlet around the islands Vlieland and Terschelling, through the Ameland Inlet to Ameland Island, from there on via the Frisian Inlet to Lauwersoog, and around Schiermonnikoog Island via the Ems-Dollard Inlet to Emden. In addition, we sampled a tidal cycle from high tide to low tide (21.05.2019) and from low tide to high tide (23.05.2019) on each day as an anchor station in the waterway at the western side of Ameland in the Ameland Inlet.

Nearly half-hourly, we continuously collected discrete surface (1.2 m depth) water samples with a bypass from the onboard flow-through FerryBox system (Petersen et al., 2011), which also provided essential physical parameters such as salinity and temperature.

For TA and DIC measurements we sampled water with overflow into 300 mL BOD (biological oxygen demand) bottles and preserved them with 300 µL saturated mercury chloride ($HgCl_2$) to stop biological activity. Each BOD bottle was filled without air bubbles and closed by using a ground-glass stopper coated in Apiezon® type M grease and a plastic cap. The samples were stored in a cool dark environment until measurements in the lab.

Water for nutrient samples was filtered through pre-combusted (4 h, 450 °C) GF/F filters and the filtrate was stored frozen in three 15 mL Falcon tubes for triplicate measurements in the lab.

To determine the total carbon (C), organic carbon (C_{org}) and nitrogen (N) concentrations in SPM and associated C_{org}:N ratios, we used pre-combusted (4 h, 450 °C) GF/F filters, which were dried after sampling at 50 °C to remove all humidity and were stored frozen afterwards until measurement.

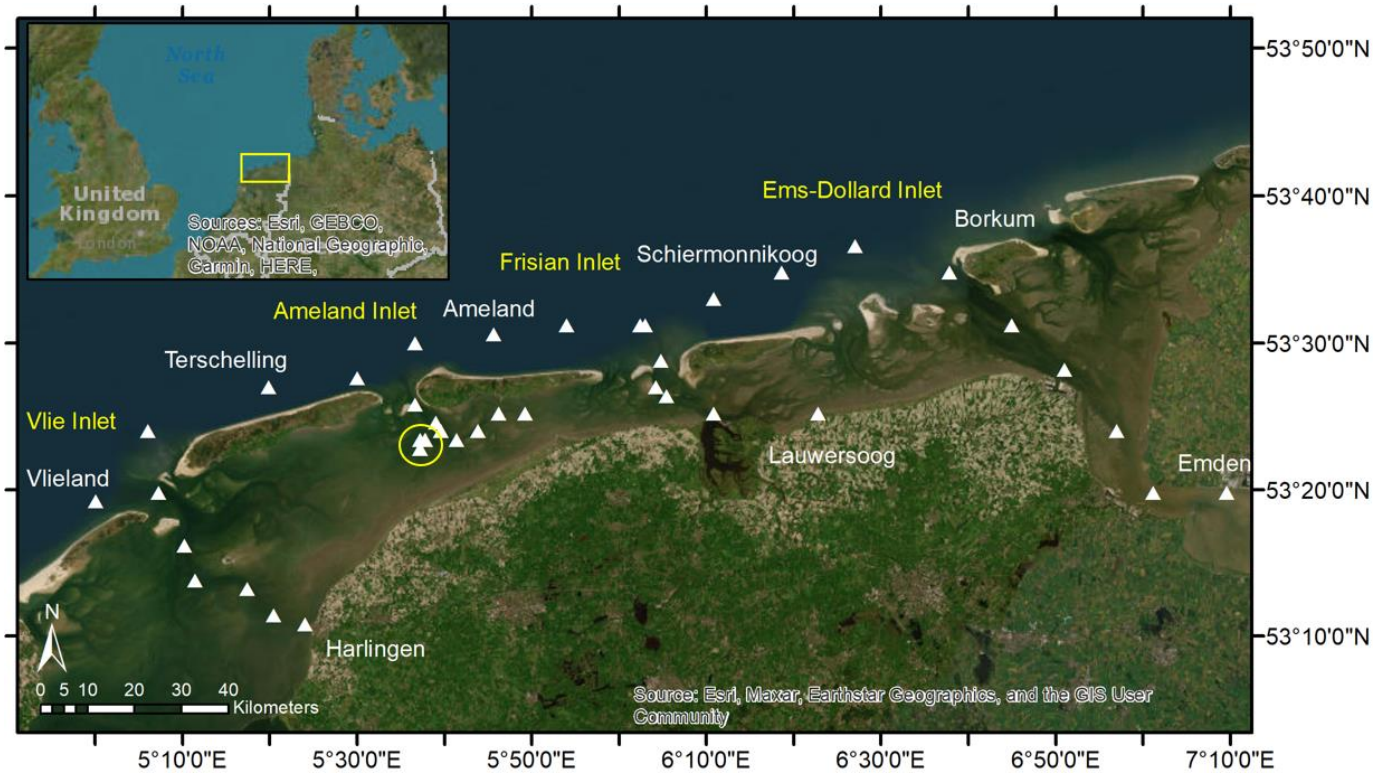

Figure 1 Sampling site in the Dutch Wadden Sea. The sampling stations around the Frisian Islands in May 2019 are visualized with white triangles. The yellow circle highlights the anchor stations for the tidal cycle sampling in the Ameland Inlet on two days. During the sampling day from low tide to high tide, we had two samples that we took slightly more western due to drifting. The island and city names are shown in white, the inlets in yellow. The tidal flats and sedimentary structures are well visible between the barrier islands and the mainland.

2.2 Carbon species analyses

The parallel analyses of TA and DIC were carried out by using the VINDTA 3C (Versatile INstrument for the Determination of Total dissolved inorganic carbon and Alkalinity, MARIANDA - marine analytics and data), which measures TA by potentiometric titration and DIC by coulometric titration with a measurement precision < 2 µmol kg^{-1} (Shadwick et al., 2011). To ensure a consistent calibration of both measurements, certified reference material (CRM batch # 187) provided by Andrew G. Dickson (Scripps Institution of Oceanography) was used.

The calcite and aragonite saturation states (Ω) and the pH were computed with the CO_2SYS program (Lewis and Wallace, 1998), using the measured parameters TA, DIC, salinity, temperature, silicate and phosphate as input variables, together with the dissociation constants from Mehrbach et al. (1973), as refit by Dickson and Millero (1987).

2.3 Nutrient analyses

The nutrients were measured with a continuous flow automated nutrient analyzer (AA3, SEAL Analytical) and a standard colorimetric technique (Hansen and Koroleff, 2007) for nitrate (NO_3^-), nitrite (NO_2^-), phosphate (PO_4^{3-}), and silicate (Si), and a fluorometric method (Kérouel and Aminot, 1997) for ammonium (NH_4^+) (Grasshoff et al., 2009).
For the C_{org} determination, filters were acidified with 1N HCl and dried overnight to remove all inorganic carbon content. Filters were measured with a CHN-elemental analyzer (Eurovector EA 3000, HEKAtech GmbH) in the Institute of Geology, University Hamburg, and calibrated against a certified acetanilide standard (IVA Analysentechnik, Germany). The standard deviations were 0.05 % for carbon and 0.005 % for nitrogen.

2.4 Data analyses

The data analyses were performed by using RStudio Version 1.3.1073 © 2009-2020 RStudio, PBC. The linear regression Model II was performed by using the "lmodel2" R package, and the plots were created with the "ggplot2" R package.

3 Results

3.1 Spatial parameter distribution

To investigate the spatial distribution of total alkalinity (TA) in the Dutch Wadden Sea and compare its general status with earlier studies (e.g., Hoppema, 1990), we observed the spatial distribution of TA and related parameters from the coastal mainland towards the open North Sea as a surface water transect.
The temperatures varied between 12 and 16 °C with higher temperatures towards the coastal mainland (Fig. 2a). Salinity was relatively stable with only minor differences varying from 28 to 33 (Fig. 2b). Lower salinities were only observed in the four sampling stations in the Ems Estuary with the minimum value of 20.25 at the most upstream station.
Spatial transect TA contents ranged from 2332 µmol kg^{-1} to 2517 µmol kg^{-1}. We observed lower contents on the oceanic, i.e., North Sea side of the Frisian Islands with somewhat higher contents around Ameland (Fig. 2c). In contrast to the oceanic side, the values were higher (> 2380 µmol kg^{-1} TA) in the Wadden Sea. Only in the Ems Estuary, the contents were even higher, with values up to 2517 µmol kg^{-1} TA at the most upstream station. Higher TA values in the Wadden Sea than in the open ocean, supporting the assumption of TA being generated in this tidal flat area.
Silicate (Si), showed a similar pattern with higher concentrations in the Wadden Sea and lower ones towards the ocean (Fig. A1). Highest concentrations were observed at the coastal mainland and in the Ems Estuary. Silicate concentrations were between 0.26 and 56.32 µmol L^{-1}. Both, the calcite and aragonite saturation states (Ω) were supersaturated in the entire study site. Values ranged from 2.3 to 4.6 for calcite (Fig. A2), and from 1.4 to 3.0 for aragonite (Table B1). Highest values were observed at the oceanic side of the barrier islands in the North Sea. The lowest values were observed near Harlingen and in the Ems Estuary. Like the calcite and aragonite saturation states, the pH values were higher in the North Sea, and lower in the

Wadden Sea and near the coastal mainland (Fig. A3). The pH values ranged from 7.86 to 8.19. The lowest values were observed near Harlingen and in the Ems Estuary. The nitrate (NO_3^-) concentrations were in a similarly low range (< 3 µmol L^{-1} NO_3^-) throughout the transect. Higher concentrations (< 6 µmol L^{-1} NO_3^-) were observed only at a few stations close to land, and maximum concentrations (< 38 µmol L^{-1} NO_3^-) were observed in the Ems Estuary (Fig. A4). DIC contents ranged from 2097 µmol kg^{-1} to 2430 µmol kg^{-1} (Fig. A5). DIC values showed a similar pattern as TA values, with higher concentrations near the coastal mainland and in the Ems Estuary, and decreasing concentrations toward the North Sea, where DIC reached minimum values.

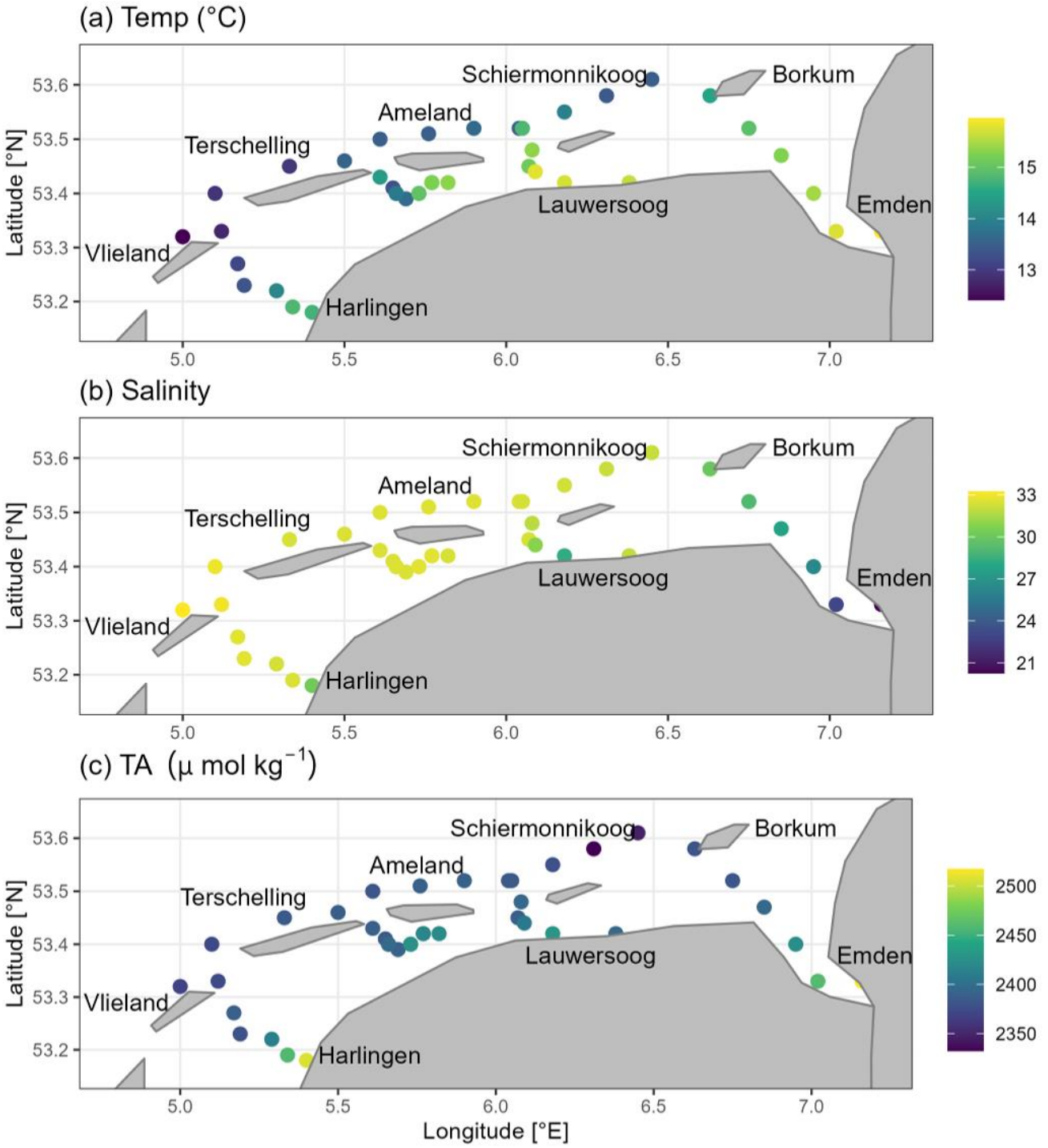

140

141 **Figure 2** Latitudinal and longitudinal distribution of a) temperature (°C), b) salinity, and c) total alkalinity (TA; µmol kg^{-1})

142 from surface water samples in May 2019.

The strong impact from the inner Ems Estuary is visible in all parameters with higher values in the outer estuary and its adjacent zones, or with lower values in case of pH and the calcite saturation state. Furthermore, we observed higher values around Ameland Island than in the western part of the transect starting from Harlingen towards the Vlie Inlet. At the oceanic side of the Vlie Inlet, the impact of the North Sea is visible through lower temperatures and higher salinities. The North Sea impact is also visible in the mixing between TA and salinity (Fig. 3). A relatively linear mixing behavior was only observed in the transect through the Ems-Dollard Inlet and Vlie Inlet, whereTA contents decreased with increasing salinities from the mainland towards the ocean (Fig. 3), identifying the Dutch Wadden Sea as a source of TA. In contrast to the TA content computed for the salinity end-member in the Ems-Dollard Inlet, we detected higher TA contents around Ameland, both at the North Sea side (Ameland NS) and the Wadden Sea side (Ameland WS), as well as in the Vlie Inlet, which further support additional TA sources in the Wadden Sea (Fig. 3). The Ameland NS and Ameland WS data clearly indicated non-conservative behavior with increasing TA contents at constant salinities.

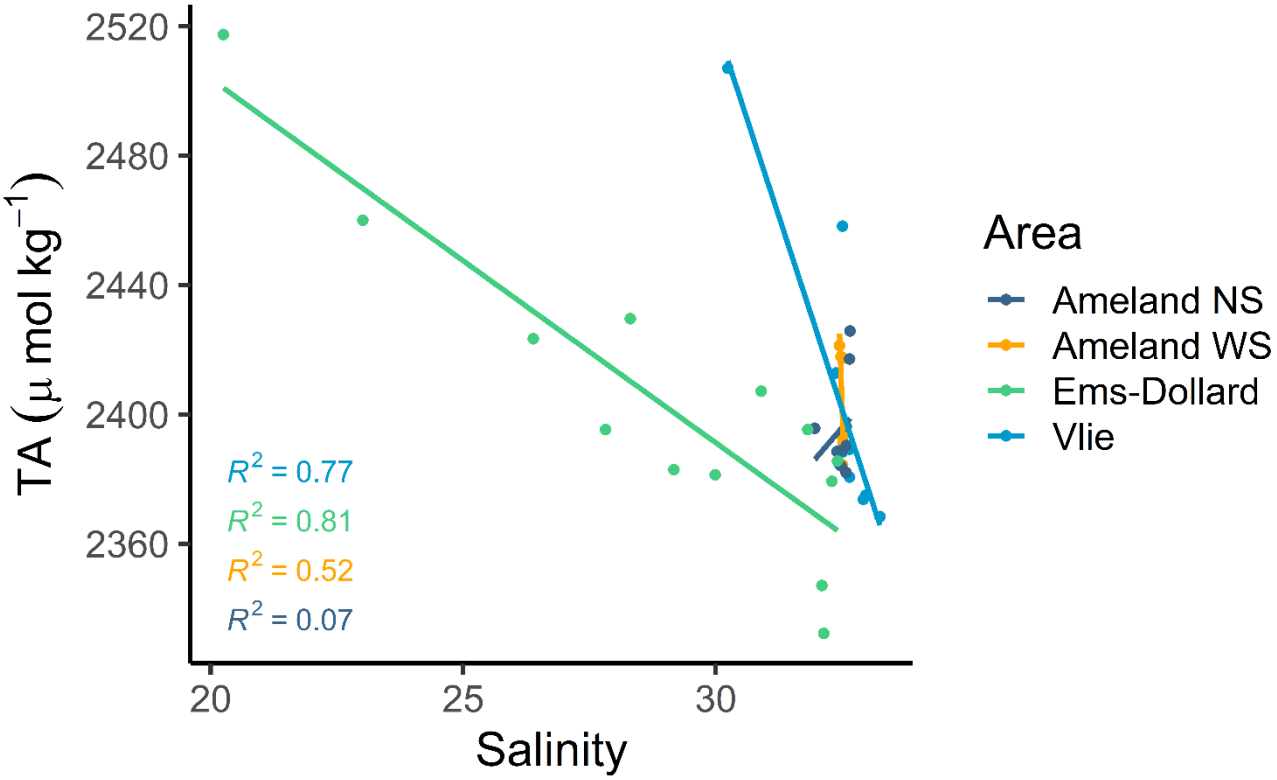

Figure 3 Mixing between total alkalinity (TA) and salinity in the oceanic side of Ameland and the Frisian Inlet (Ameland NS), in the Wadden Sea site of Ameland (Ameland WS), around Schiermonnikoog and in the Ems-Dollard Inlet, and in the Vlie Inlet.

3.2 Tidal cycle

To estimate TA generation in the Dutch Wadden Sea, to shed light on potential TA sources, and to estimate the potential TA amount that is exported to the North Sea, we observed a tidal cycle at an anchor station in the Ameland Inlet on two days during flood tide and ebb tide, respectively. Here, the focus is on ebb tide data that we used to identify patterns in the several biogeochemical parameters in off running water (Table B1). The salinity observations allow us to exclude addition by mixing with freshwater sources, since the salinity was constant between 32.50 and 32.52 (Table B1). Salinity values were in the range of saline waters like water of the North Sea.

During ebb tide, TA ranged from high tide with 2387 µmol kg^{-1} TA to low tide with 2438 µmol kg^{-1} TA (Fig. 4a). We identified an increase of 51.6 µmol kg^{-1} TA (ΔTA) over a duration of 6.8 h during ebb tide, resulting in a TA increase of 7.6 µmol kg^{-1} h^{-1} TA at the sampling location.

DIC contents were similar to TA with minimum values at high tide (2172 µmol kg^{-1} DIC) and highest values (2273 µmol kg^{-1} DIC) at low tide. During ebb tide, we observed an increase of 101.3 µmol kg^{-1} DIC (ΔDIC) resulting in a DIC increase of 14.9 µmol kg^{-1} h^{-1} DIC (Fig. 4b). DIC increased almost twice as much as TA.

Nitrate concentrations approached seawater concentrations with an observed minimum of 1.26 µmol L^{-1} NO_3^- and a maximum of 2.17 µmol L^{-1} NO_3^- (Fig. 4c). During ebb tide, nitrate slightly increased by 0.92 µmol L^{-1} NO_3^- (ΔNO_3^-), resulting in a nitrate increase of 0.13 µmol L^{-1} h^{-1} NO_3^-.

In silicate, a similar pattern with low values (1.8 µmol L^{-1} Si) at high tide and increasing concentrations during ebb tide to a maximum of 11.2 µmol L^{-1} Si was detected. The silicate increase (ΔSi) of 9.4 µmol L^{-1} Si resulted in a silicate increase of 1.4 µmol L^{-1} h^{-1} Si during ebb tide (Fig. 4d).

Ammonium increased from 3.47 µmol L^{-1} NH_4^+ to 6.22 µmol L^{-1} NH_4^+ during ebb tide (Fig. 4e). We observed an ammonium increase (ΔNH_4^+) of 2.74 µmol L^{-1} NH_4^+ resulting in an increase of 0.4 µmol L^{-1} h^{-1} NH_4^+.

The calcite and aragonite saturation states had maximum values (Ω_{Ca} = 3.8, Ω_{Ar} = 2.4) at high tide and decreased to their minimum (Ω_{Ca} = 3.1, Ω_{Ar} = 2.0) during ebb tide (Fig. 4f, Table B1). The maximum at high tide indicated the influence of the North Sea that decreased during the ebb.

Like omega, the pH had maximum values (8.07) at high tide and decreased to a minimum (7.93) during ebb tide (Fig. 4g).

C_{org}:N ratios of SPM increased during ebb tide (Fig. 4h). A minimum C_{org}:N ratio of 5.6 was observed around high tide and increased to a maximum of 13.0 during ebb tide. Simultaneously, the SPM concentration increased during ebb tide, from 12.8 mg L^{-1} SPM to a maximum of 82.4 mg L^{-1} SPM at the second last station (Table B1).

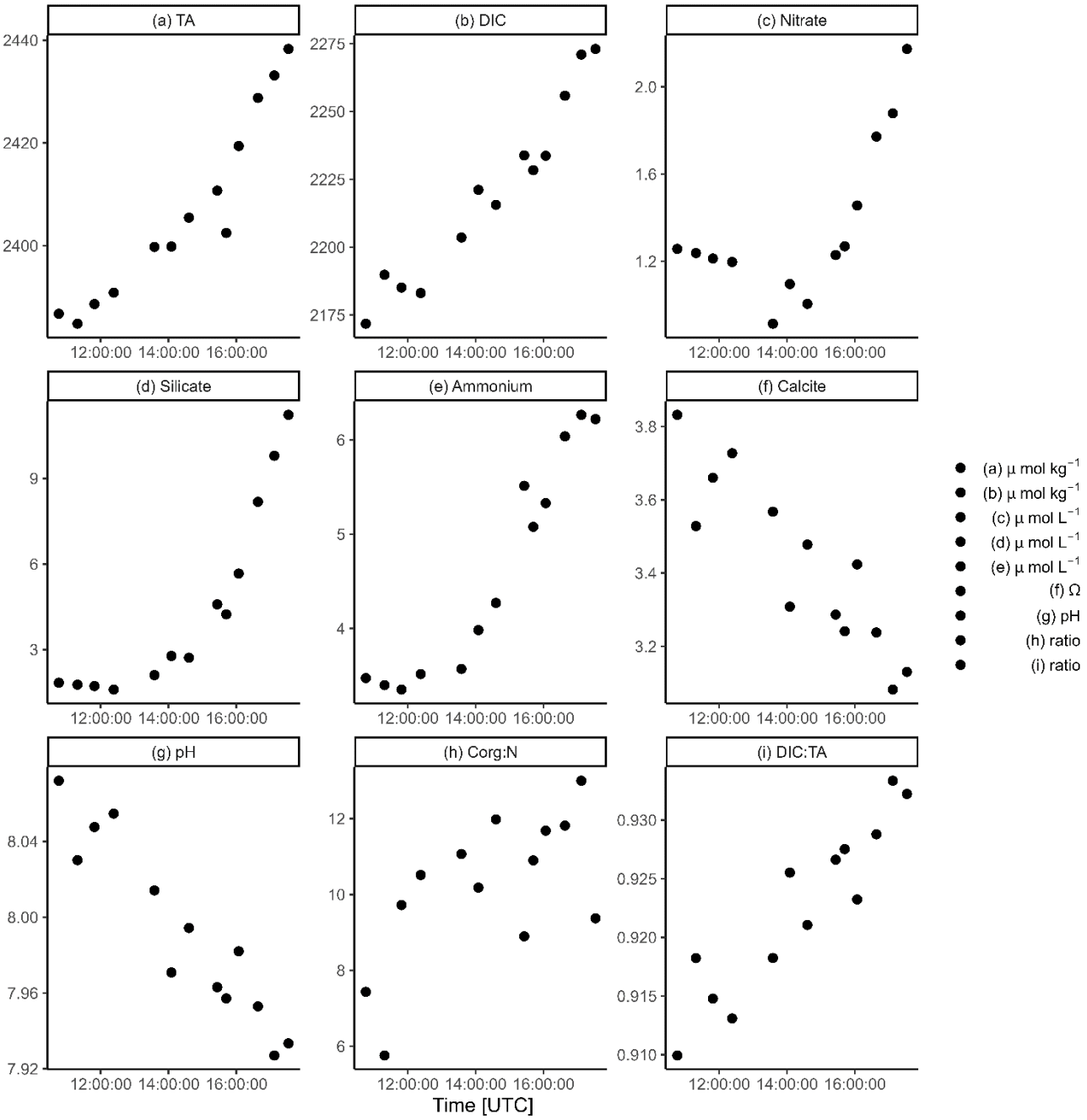

187

188 **Figure 4** Tidal cycle from high tide to low tide. Temporal distribution of a) total alkalinity (TA), b) dissolved inorganic
189 carbon (DIC), c) nitrate, d) silicate, e) ammonium, f) calcite saturation state (Ω), g) pH, h) C_{org}:N ratio of SPM, and i)
190 DIC:TA ratio. Note the different y-axes.

3.3 TA generation

The Dutch Wadden Sea is exposed to strong tidal forcing by the North Sea leading to a bi-diurnal exchange of water. The strong tidal forcing induces a strong benthic-pelagic coupling. Many studies support that the outflowing water exports material from the sediment (e.g., Billerbeck et al., 2006;Røy et al., 2008). To support our assumption of a sediment source of TA, we further investigated potential TA sources.

For a first rough estimate of a maximum TA export during ebb tide, we used the observed TA increase (ΔTA) of 51.6 µmol kg^{-1} TA during ebb tide (in the Ameland Inlet), and the tidal prism of 478 $*10^6$ m^3 of the Ameland Inlet (Louters and Gerritsen, 1994). With this estimate, we obtained a rough TA export on the order of 23.9 mol TA during ebb tide from the Ameland Inlet into the North Sea. With a tidal duration of 6.8 h, the estimated TA export of 23.9 mol would result in a TA export of 3.5 mol h^{-1} TA.

Based on the correlation of TA and silicate (R^2 = 0.93), and on the nonlinear relation between both, TA and salinity (R^2 = 0.32), as well as silicate and salinity (R^2 = 0.21), we were able to determine whether TA originates in this part of the Dutch Wadden Sea or is carried by river runoff. Both TA and silicate increased almost proportionally during ebb tide, pointing to the same origin (Fig. 5b). The non-conservative behavior of TA over salinity and silicate over salinity rules out any sources due to freshwater dilution and river runoff (Table B1).

To further elucidate potential TA sources in the Dutch Wadden Sea, we correlated TA with DIC, silicate, nitrate, and ammonium from high tide to low tide (Fig. 5). The first four samples on the left side of the plots in Fig. 5 show values probably at the tipping point of high tide, whereby we recommend neglecting these samples in the interpretation of ebb tide samples.

First, the correlation between TA and DIC reveals the ratio between anaerobic and aerobic processes, which identifies a strong positive correlation between DIC and TA (R^2 = 0.93) with TA contents higher than DIC contents (Fig. 5a). However, even with contents of TA higher than DIC, the slope of 1.87 indicated DIC release excess with an increase in DIC (ΔDIC = 101.3 µmol kg^{-1}) almost twice as high as TA (ΔTA = 51.6 µmol kg^{-1}) (Fig. 5a). This may be caused by strong CO_2 production due to high aerobic OM degradation, or uptake from the atmosphere due to water movement by tidal forcing. The TA increase can be fueled by various processes which we will discuss below. We detected an almost linear positive correlation of increasing TA and silicate (R^2 = 0.93) during ebb tide, supporting the pore water outflow (Fig. 5b). A stronger influence of the pore water with ongoing ebb tide is indicated by increasing values. The positive correlation between nitrate and TA (R^2 = 0.67) (Fig. 5c) was less strong than the correlations between TA and DIC, and TA and Si, which could be traced back on an effect of the first four samplings as mentioned above. In the remaining samples, the increasing nitrate and TA contents suggest a stronger effect of TA generation than nitrate production.

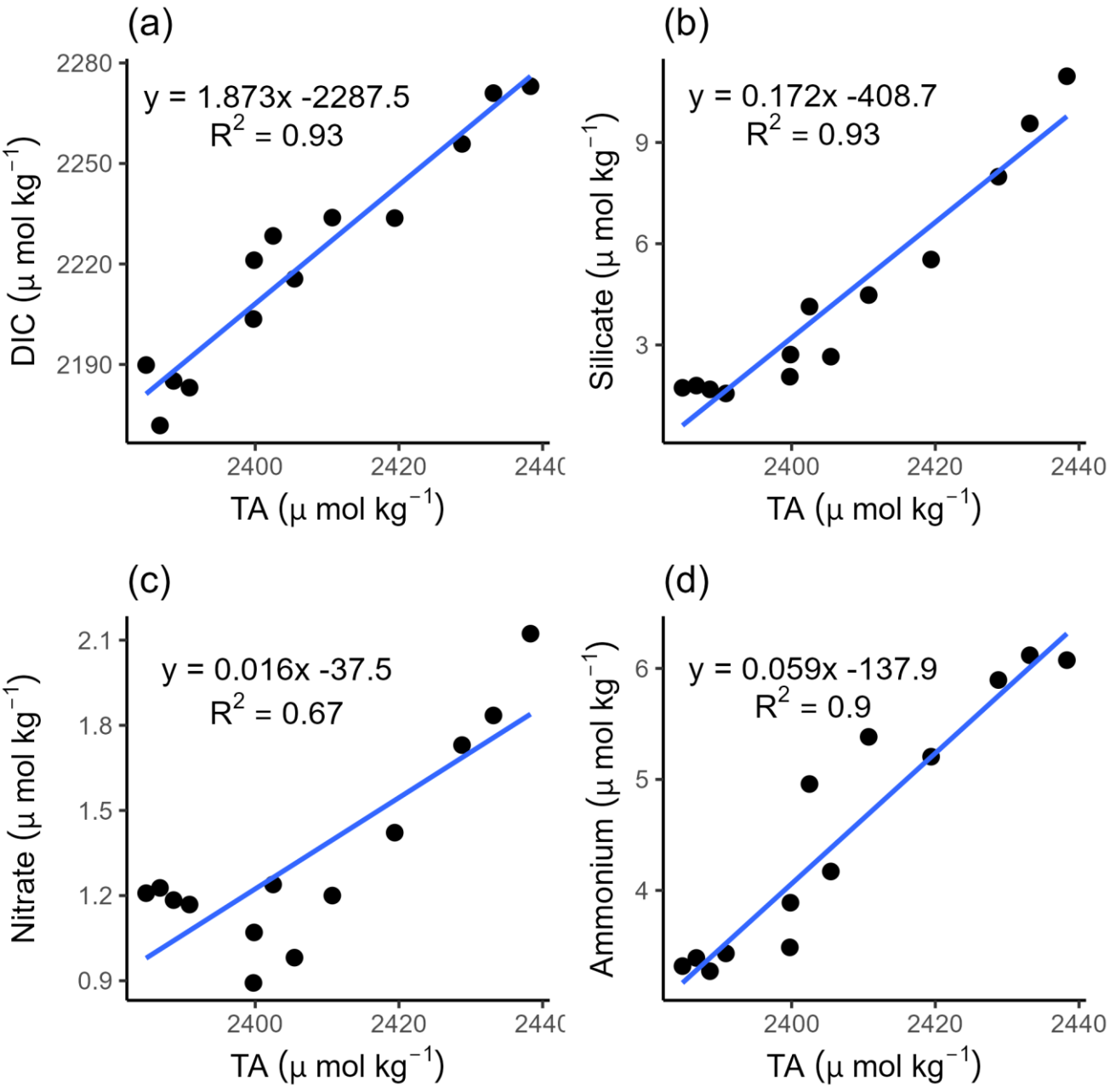

220

221 **Figure 5** Correlations of TA with a) dissolved inorganic carbon (DIC), b) silicate, c) nitrate, and d) ammonium during ebb
222 tide in the Ameland Inlet.

4 Discussion

4.1 Spatial TA variability

Hoppema (1990) reported TA distributions in the westernmost part of the Dutch Wadden Sea around the barrier islands Texel, Vlieland, and Terschelling. He focused on the tidal basins drained by the tidal inlets Marsdiep and Vlie located more to the west than our sampling stations (not visible on the map). Hoppema (1990) did not observe an increase of salinity in the Wadden Sea from the freshwater source towards the ocean and associated this to the influence of tidal differences and an arbitrary sampling scheme. The presence of seawater in the Dutch Wadden Sea and on the tidal flats is supported by our transect data, which show relatively high salinities at coastal North Sea level. Brackish salinities were only detected in the large Ems Estuary, which receives high discharges of freshwater from the river Ems, and also close to Harlingen and Lauwersoog, which have direct freshwater inflows by smaller rivers and streams. The absence of clear salinity gradients in this part of the Dutch Wadden Sea suggest that most of the IJsselmeer discharge was exchanged with the North Sea through the Marsdiep.

The spatial TA data by Hoppema (1990), show lower TA contents at stations with more freshwater influence and higher TA contents in the tidal inlets. The data of this study also show high TA contents in the tidal inlets, suggesting TA generation in sediments, which is fueled by high imports of nutrients and OM (Van Beusekom and De Jonge, 2002). The even higher TA contents at stations with lower salinities close to the mainland observed in this study also show the influence from the catchment area on the coast, and TA generation in the shallow sediments near the coast. In May (1986), Hoppema's (1990) data showed TA contents ranging between 2319 and 2444 µmol kg^{-1} TA at salinities between 18.62 and 29.17, while our lowest observed TA content was 2332 µmol kg^{-1} TA at a salinity of 32.14, and our highest TA content was 2517 µmol kg^{-1} TA at a salinity of 20.25 close to the coastal mainland. Comparing both studies, one can say that the general level of TA was in a similar range.

A conservative mixing between TA and salinity is only visible in the Ems-Dollard Inlet and the Vlie Inlet (Fig. 3). The conservative mixing in the Vlie Inlet can be explained by the fact that more North Sea water pass through the deeper inlets and transport more seawater towards the coast. The Vlie Inlet has the highest average tidal prism and is the second largest inlet after the Marsdiep Inlet in the Dutch Wadden Sea (Elias et al., 2012). Similar to our findings, Hoppema (1990) noted a linear mixing of TA and salinity in the Vlie Inlet, and suspected a lower freshwater contribution there as well.

In the Ems-Dollard Inlet, conservative mixing was observed indicating minor contributions from other sources. In a previous study, Norbisrath et al. (2023) observed very high TA contents and TA generation in the upper tidal river of the highly turbid Ems Estuary, which may explain the high levels of TA in the estuary (at low salinities) observed in this study.

Hoppema (1990) also identified varying TA contents within the Dutch Wadden Sea and related these to different sinks and sources. TA sinks can be calcium carbonate ($CaCO_3$) precipitation, or extraction of seawater carbonate by mollusks (e.g., Chen and Wang, 1999;Hoppema, 1990). Variable freshwater inflows can either serve as a sink or a source (e.g., Chen and Wang,

1999;Hoppema, 1990). Other TA sources can be $CaCO_3$ dissolution, anaerobic metabolic processes in the sediment, or erosion of TA enhancing sediments (e.g., Hoppema, 1990;Chen and Wang, 1999).

Since we observed constant marine salinities (> 30), and higher TA values in the Dutch Wadden Sea than in the North Sea, we exclude TA sinks and focus only on TA sources. According to Hoppema (1990), the main causes for TA variations in the Dutch Wadden Sea were freshwater inflows and sources in the sediment. In our study, freshwater inflows with high TA contents were only observed in the Ems Estuary and Ems-Dollard Inlet, but not around the islands and the tidal flats. For a further TA source identification in the Dutch Wadden Sea, we investigated the TA variability during a tidal cycle close to Ameland.

4.2 Determination of TA generation

Burt et al. (2016) and Schwichtenberg et al. (2020) assumed TA generation in the Wadden Sea as an important source for the North Sea's carbon storage capacity. Here, we want to further identify TA generation and potential TA sources.

In a study from the early 1990s, Hoppema (1993) observed a tidal cycle in the Marsdiep in May and September. Focusing on TA, DIC, and oxygen, he also observed increasing TA values during ebb tide and assumed the tidal flats and discharging rivers and canals as TA sources. Our present TA data and the historical TA data show no large differences in the range of values observed during a tidal cycle. However, an in-depth interpretation and comparison of both data sets would exceed the capacity of these data, leading us to focus on TA generation during our cruise.

Our observation of a TA generation of 7.6 µmol kg^{-1} h^{-1} TA during ebb tide supports the assumption of the Wadden Sea being a TA source for the North Sea. With the tidal prism of the Ameland Inlet estimated by Louters and Gerritsen (1994), we estimated an upper bound TA export from the Dutch Wadden Sea into the North Sea on the order of 23.9 mol TA during ebb tide (3.5 mol h^{-1} TA) between spring and summer. This TA export is a rough maximum estimate, because some waters in the main tide channels have no direct contact to the areas of the tidal flats. Schwichtenberg et al. (2020) assumed an annual export of 10 to 14 Gmol yr^{-1} TA for the entire Dutch Wadden Sea. However, an inclusion of our TA export into the model used by Schwichtenberg et al. (2020) would be unreliable, since our TA export based only on one tidal observation (personal communication J. Pätsch, 2022). To test whether the observed TA generation matches their suggested TA export, more observational data are required. We suggest at least seasonal observational data in order to run the model and gain a representative result (personal communication J. Pätsch, 2022) as future work.

4.3 TA source attribution

4.3.1 Local sediment outwash

In order to gain further insight into potential sources of TA, we included nutrients in our investigation. The main focus was on silicate that we used as a natural tracer since it is not directly provided anthropogenically and allowed us to determine the silicate source (Van Der Zee and Chou, 2005). We identified a silicate increase of 1.4 µmol L^{-1} h^{-1} Si during ebb tide. Silicate

originates from dissolution of diatoms and pore water exchange in the Wadden Sea (Van Bennekom et al., 1974;Van Der Zee and Chou, 2005). Here, we relate the silicate increase to pore water exchange, because it markedly increased during ebb tide. This assumption is supported by Van Bennekom et al. (1974), who suggested silicate diffusion from interstitial water in the sediment as potential source, since very high silicate concentrations were found in deeper sediment layers (Rutgers van der Loeff, 1974). Due to the absence of large estuaries nearby and salinity consistently being above 32, we exclude freshwater runoff as a major silicate source. This can be supported by the relation between silicate and salinity in which we observed a non-conservative behavior (Table B1). Since TA behaves also non-conservative relative to salinity (Table B1), the silicate observations support the occurrence of TA sources in the tidal flats of the Wadden Sea.

Submarine groundwater discharge (SGD) was identified as a source for nutrient fluxes in tidal flat ecosystems in previous studies (e.g., Billerbeck et al., 2006;Røy et al., 2008;Santos et al., 2021;Waska and Kim, 2011;Wu et al., 2013). Waska and Kim (2011) identified strong SGD contributing up to 50 to 70 % of the nutrient fluxes that fuel primary production in a tidal embayment (Hampyeong Bay) in southwest Korea. In May, they observed low salinities indicating freshwater. However, in September they observed constant marine salinities referring them to be exclusively composed of recirculating seawater. Since we constantly observed marine salinities, we suspect that recirculating marine groundwater enriched with nutrients act as a source for our observed increasing TA and nutrients parameters.

TA generation in tidal flats was also observed by Faber et al. (2014), who focused on a large macro tidal embayment in southern Australia. They also found increasing TA values during ebb tide, associated the TA increase with a higher fraction of pore water, and determined the tidal cycle as the controlling force for pore water exchange. Their findings and the observed silicate outwash support our assumption that TA is generated in the sediments of the tidal flats and is washed out during ebb tide. In addition, we exclude lateral advected signals from more western regions as the Vlie Inlet, since the TA contents in the surface transect samples in the Vlie Inlet (except of the two samples close to the coastal mainland near Harlingen) were in the same range as the other observed TA contents and were below the increasing TA contents during ebb tide. Both increases in TA and silicate are clearly tidal signals, and we clearly identify TA generation in the sediments of the tidal flats here as local TA sources.

4.3.2 TA generating processes

The observed TA generation of 7.6 µmol kg^{-1} h^{-1} TA and the silicate increase of 1.4 µmol L^{-1} h^{-1} Si indicated an excess of TA given a TA:silicate ratio of 2:1 (Marx et al. 2017), and under the condition of silicate being bound in minerals, which would then account for a TA generation of 2.8 µmol kg^{-1} h^{-1} TA. However, when silicate occurred dissolved in water it does not contribute to TA generation (Meister et al., 2022). A TA excess related to silicate was also observed in the correlation between TA and silicate (Fig. 5b). Since we observed more TA generated than silicate being washed out, other biogeochemical processes must be responsible for the TA generation in the sediments of the tidal flats in the Dutch Wadden Sea.

With the observed omega values, we exclude $CaCO_3$ dissolution as TA source in the overlying water, since the omega values were clearly supersaturated with $\Omega > 1$(Fig. 4f, Table B1). The continuous calcite supersaturation nicely indicated the inflow and dominance of North Sea water during the flood, with omega values similar to previously observed North Sea values ($\Omega \sim$ 3.5 to 4) (Charalampopoulou et al., 2011;Carter et al., 2014). However, because of the Ω supersaturation of the overlying water and a lack of pore water data, we were unable to determine if TA generation by $CaCO_3$ dissolution occurs in deeper sediment layers. There, $CaCO_3$ dissolution can only be driven metabolically, when CO_2 is produced during OM remineralization, or when reduced compounds that were previously produced during anaerobic processes are oxidized and lead to undersaturation with respect to carbonates (Brenner et al., 2016;Jahnke et al., 1994).

A more detailed interpretation of ΔDIC, ΔTA, and various nutrient ratios, further narrows down the potential sources of TA generation in the sediments and used an upper bound estimate for $CaCO_3$ dissolution. The correlation of DIC and TA reveals an excess of released DIC compared to TA (Fig. 5a), as indicated by the slope of 1.87, while we observed an increase in DIC (ΔDIC) almost twice as high as in TA (ΔTA). The high ΔDIC points to high aerobic OM degradation and remineralization, resulting in high CO_2 export. High aerobic OM degradation was also previously observed in the heterotrophic Wadden Sea (e.g., De Beer et al., 2005;Van Beusekom et al., 1999), assuming an OM degradation and remineralization occurring in the water and sediment in about equal parts (Van Beusekom et al., 1999). High OM degradation is also indicated by the increasing C_{org}:N ratios of SPM during ebb tide (Fig. 4h, Table B1). Because we observed constant coastal North Sea salinities, we rule out freshwater runoff and terrestrial signals as source for the increasing C_{org}:N ratios of SPM. We assume that fresh OM is rapidly degraded in the water column, and the older OM settles on and in the sediment where the degradation continuous and where it is resuspended by the water exchange with outflowing water. Therefore, we assume that the increase of SPM concentrations and their C_{org}:N ratios is an indicator for older and more refractory OM. The increase in TA contents point to anaerobic processes, $CaCO_3$ dissolution, or a combination thereof as TA sources occurring in the sediments.

For the upper bound estimate, we assumed $CaCO_3$ dissolution in the sediments with the DIC:TA ratio of 1:2 as source of TA. Considering this ratio and the observed ΔTA of 51.6 µmol kg^{-1} TA, a potential ΔDIC of 25.8 µmol kg^{-1} DIC of the observed ΔTA would be produced by $CaCO_3$ dissolution. The remaining potential 75.5 µmol kg^{-1} DIC (101.3 – 25.8 µmol kg^{-1} DIC) of the observed (ΔDIC) could then be produced by OM degradation and remineralization, and would, using the expected Redfield ratio of C:N (6.6), correspond to an estimated potential dissolved inorganic nitrogen (DIN) production of 11.4 µmol kg^{-1} DIN. However, this estimated potential DIN production (11.4 µmol kg^{-1} DIN) of OM degradation and remineralization exceeded the observed increase of ΔDIN (3.97 µmol L^{-1} DIN; Table B1, sum of NO_3^-, NO_2^- and NH_4^+) during ebb tide. With this estimation and the assumption that all DIN produced is released and thus lost, TA is probably produced by $CaCO_3$ dissolution and anaerobic metabolic processes other than denitrification in the sediment. In addition to that, and with a N-focused perspective, the DIN loss also hints to the occurrence of other processes that consume nitrogen species but have no net effect on TA, such as anammox and coupled nitrification-denitrification (Hu and Cai, 2011;Middelburg et al., 2020). The suggested DIN loss can be supported by considering the marine DIN:Si ratio, which is supposed to be 1:1 (Brzezinski, 1985). We

observed DIN:Si ratios decreasing from 2.7 to 0.8 from high tide to low tide. The decreasing ratios show that both parameter concentrations increased during ebb tide, whereby DIN concentrations increased lower than silicate concentrations. We observed a silicate excess with respect to DIN at the end of ebb tide, supporting the DIN loss.

Denitrification, the anaerobic irreversible reduction of NO_3^- to N_2 that generates 0.9 mole TA by using 1 mole NO_3^- as electron acceptor (Chen and Wang, 1999) is a net TA source. Denitrification depends on the supply of nitrate, which seasonally varies (Van Der Zee and Chou, 2005 and references therein). Generally, nitrate is depleted in summer due to high turnover rates and occurs in higher concentrations in winter (Kieskamp et al., 1991;Jensen et al., 1996;Van Der Zee and Chou, 2005). This seasonality lead to denitrification rates also being lower in summer and higher in winter (Kieskamp et al., 1991;Jensen et al., 1996). In previous studies, Faber et al. (2014) identified denitrification as a minor source of TA due to low denitrification rates, and also Kieskamp et al. (1991) observed low denitrification rates in the Wadden Sea, with low nitrate concentrations (< 2.5 µmol L^{-1}) in the overlying water. We observed nitrate concentrations (< 2.17 µmol L^{-1}) lower than the concentration sufficient for denitrification assumed by Kieskamp et al. (1991). Therefore, we do not exclude denitrification, but suspect it as a minor source of TA in the Dutch Wadden Sea at least in spring and summer due to the seasonal lack of nitrate. Thomas et al. (2009) detected TA seasonality in the southern bight of the North Sea, which is also influenced by the TA generation in the Wadden Sea. We support their findings of lowered TA generation by denitrification in late spring and early summer. In addition, the calculated potential DIN excess compared to the observed DIN not only hints to other N consuming processes that have no effect on TA, but also suggests that allochthonous nitrate would be needed to fuel the TA increase by denitrification. In addition, the albeit low availability of nitrate indicates to predominantly aerobic metabolic activity during the time of our observations, which is in line with earlier studies reporting an enhanced relevance of anaerobic activity later in summer (Luff and Moll, 2004;Thomas et al., 2009).

Another source of TA in sediments is aerobic OM respiration with the associated formation of ammonium while consuming H^+ (Blackburn and Henriksen, 1983;Berner et al., 1970;Brenner et al., 2016). The observed increasing ammonium concentrations (Fig. 4e) could be associated with aerobic OM degradation leading to ammonium formation. The resulting ammonium formation in the upper oxygenated sediment layers would increase DIC by the production of CO_2, and increase TA by the consumption of H^+ (Fig.5) (Brenner et al., 2016). In sediments, the production of one mole ammonium (from ammonia) would then generate one mole TA (Berner et al., 1970;Meister et al., 2022). In contrast, in the water column, the aerobic respiration of OM produce CO_2 and increase DIC, also visible in decreasing pH values (Fig. 4g), but consume TA and would not produce ammonium (Chen and Wang, 1999). Therefore, aerobic OM respiration in the water column could only explain the higher increase in DIC than in TA, but not the simultaneous increase in TA and ammonium (Fig. 5). Based on this, we assume that OM respiration associated with TA generation occurs in the sediments, leading to TA and DIC generation and also to ammonium production, being washed-out during ebb tide. The produced ammonium is then also accessible for nitrification that produces nitrate. A slightly increased nitrate concentration in the most upper sediment layers was observed by Beck et al. (2008a) in the German Wadden Sea. This observation, a potential nitrate reservoir, nitrate production due to OM

degradation and nitrification occurring in the upper oxygenated sediment layers (Martin and Sayles, 1996), or a combination thereof could explain the observed low increasing nitrate concentrations during ebb tide. However, as we rule out terrestrial nitrate imports as nitrate source here, the simultaneous increase of TA and nitrate is noticeable for us, because nitrification consumes TA (Brenner et al., 2016). We assume that potential nitrification has a minor effect on TA, since we observed only low nitrate concentrations and a really low increase of nitrate compared to the increase of ammonium and TA during ebb tide. Low nitrate concentrations resulting in a reduced availability of bound oxygen, i.e., electron acceptors. This promotes the occurrence of other anaerobic processes of the redox system to generate TA in the deeper, anoxic sediment layers in the Dutch Wadden Sea, such as sulfate and iron reduction.

Sulfate reduction followed by iron reduction and the formation and burial of pyrite are net sources of TA, since TA consumption by reoxidation is excluded when buried in sediments (Berner et al., 1970;Faber et al., 2014). Whether these processes contribute to TA generation in the deeper sediments of the Dutch Wadden Sea cannot be further identified without the necessary data. However, sulfate reduction was also mentioned as source of TA by Thomas et al. (2009). The temporary slight appearance of noticeable sulfuric odor could be another indirect indicator for the occurrence of sulfate reduction. In previous studies of tidal flats in the German Wadden Sea, Beck et al. (2008a);(2008b) observed increasing TA contents with depth and identified sulfate reduction as the most important process for anaerobic OM remineralization in pore water cores. Sulfate reduction releases 1.14 mole TA with the oxidation of one mole carbon of POC , and iron reduction releases 8.14 mole TA with the oxidation of one mole carbon of POC, indicating that both processes are large sources of TA generation (Brenner et al., 2016), but further studies are needed to support this.

A strict comparison of the northern and the western parts of the Wadden Sea is difficult because the areas vary in terms of OM import and eutrophication effects (Van Beusekom et al., 2019), sediment composition, and extent between the barrier islands and the mainland, all of which influence the occurrence and interaction of biogeochemical processes (Schwichtenberg et al., 2020). The area characteristics of the northern and western Wadden Sea differ especially in terms of OM turnover being lower in the norther Wadden Sea. A previous study by Brasse et al. (1999) identified high TA and DIC contents in the sediment of the North Frisian Wadden Sea and identified $CaCO_3$ dissolution and sulfate reduction as major TA sources, which is consistent with our findings.

5 Conclusion

The Dutch Wadden Sea is a unique and highly dynamic ecosystem. While observing the spatial TA distribution and TA generation in the Dutch Wadden Sea, we detected higher TA values than in the North Sea and identified the Dutch Wadden Sea clearly as a TA source for the North Sea's carbonate system. Compared to previous studies (Hoppema, 1990, 1993), the TA values we observed were in a similar range, with high TA values in the tidal basins. Beside the need for seasonal

observations, future work should also focus on the tidal end-members to better understand the general and seasonal influence of freshwater inflows on the TA status in the Dutch Wadden Sea.

By observing salinity and using silicate as a tracer, we excluded freshwater dilution and river runoff as TA sources on the tidal flats, and instead, identified local outwash from the sediments as sources of TA. Aerobic, metabolic processes such as $CaCO_3$ dissolution and ammonium formation seem to dominate TA generation in the upper oxic sediment layers and the overlying water, while anaerobic, metabolic processes such as denitrification, sulfate and iron reduction are potential TA sources in the deeper anoxic sediment layers. However, in spring and early summer, denitrification seems to play a minor role in generating TA in the sediments of the Dutch Wadden Sea due to seasonality and associated limited nitrate availability.

6 Appendices

Appendix A

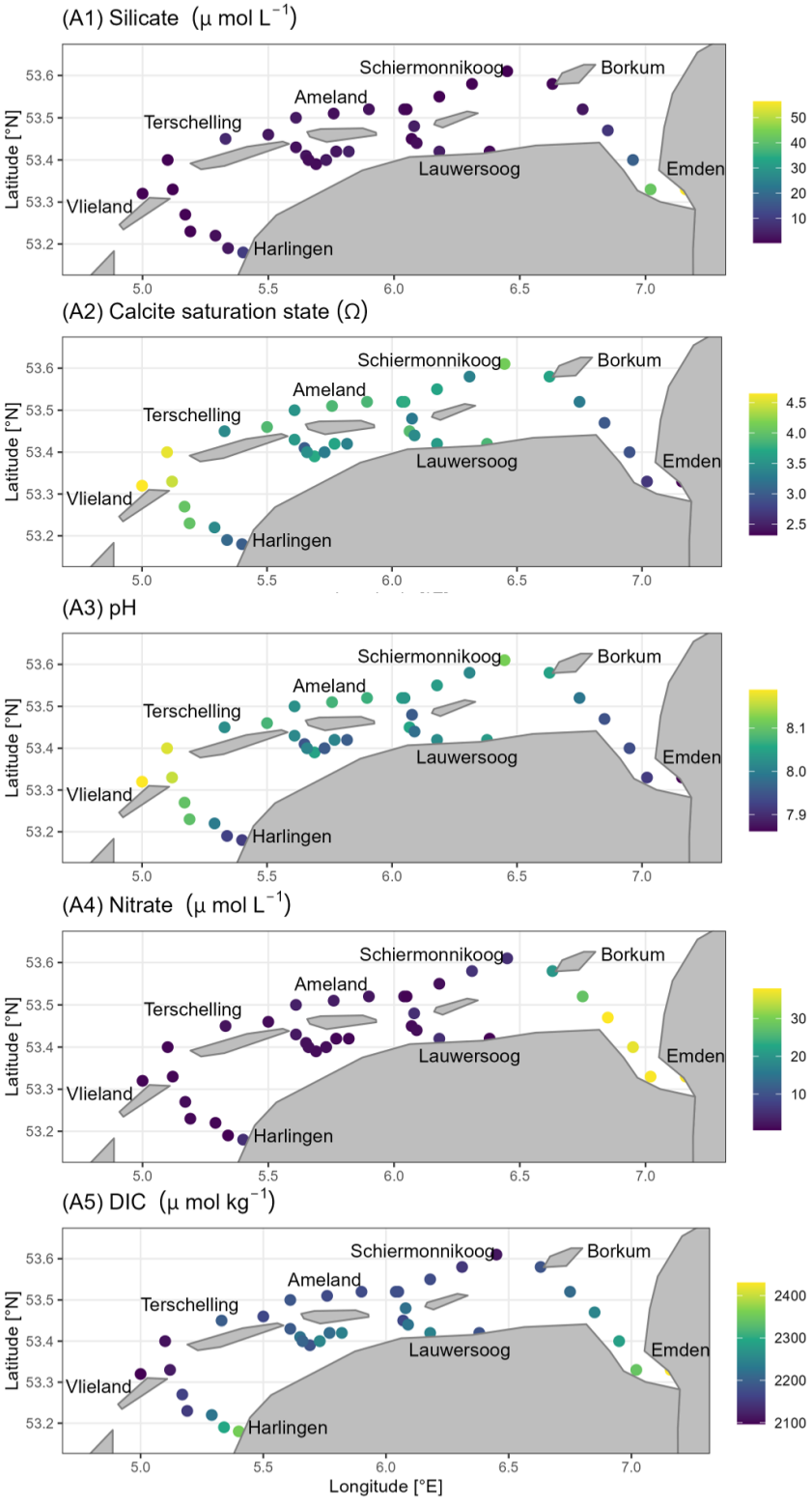
(A1) Silicate (μ mol L^{-1})
(A2) Calcite saturation state (Ω)
(A3) pH
(A4) Nitrate (μ mol L^{-1})
(A5) DIC (μ mol kg^{-1})
Schiermonnikoog
Borkum
Ameland
Terschelling
Lauwersoog
Emden
Vlieland
Harlingen
Latitude [°N]
Longitude [°E]
53.6
53.5
53.4
53.3
53.2
5.0
5.5
6.0
6.5
7.0
50
40
30
20
10
4.5
4.0
3.5
3.0
2.5
8.1
8.0
7.9
2400
2300
2200
2100

427

Figure A Latitudinal and longitudinal distribution of A1) silicate (Si; µmol L^{-1}), A2) calcite saturation state (Ω), A3) pH, A4) nitrate (NO_3^-; µmol L^{-1}), and A5) dissolved inorganic carbon (DIC; µmol kg^{-1}) from surface water samples in May 2019.

Appendix B

Table B1 Tidal cycle sample parameter during ebb tide. Sample no. 545 is the first sample at high tide and sample no. 557 is the last sample at ebb tide on May 21st 2019. Shown are rounded up values of temperature (Temp), salinity (Sal), total alkalinity (TA), dissolved inorganic carbon (DIC), silicate (Si), nitrate (NO_3^-), nitrite (NO_2^-), ammonium (NH_4^+), dissolved inorganic nitrogen (DIN), the amount of carbon (C) and organic carbon (C_{org}) of SPM, the amount of nitrogen (N) of SPM, the calcite (Ca) and aragonite (Ar) saturation states, the pH, and phosphate (PO_4^{3-}) per sample.

Sample No.	Temp [°C]	Sal	TA [µmol kg^{-1}]	DIC [µmol kg^{-1}]	Si [µmol L^{-1}]	NO_3^- [µmol L^{-1}]	NO_2^- [µmol L^{-1}]	NH_4^+ [µmol L^{-1}]
545	13.26	32.52	2387	2172	1.84	1.26	0.19	3.47
546	13.25	32.52	2385	2190	1.77	1.24	0.19	3.40
547	13.28	32.52	2389	2185	1.72	1.21	0.19	3.35
548	13.38	32.52	2391	2183	1.6	1.19	0.19	3.52
549	14.32	32.50	2400	2204	2.11	0.91	0.25	3.57
550	14.61	32.50	2400	2221	2.78	1.09	0.29	3.98
551	14.64	32.51	2405	2216	2.72	1.01	0.29	4.27
552	14.73	32.51	2411	2234	4.59	1.23	0.34	5.51
553	14.77	32.51	2402	2228	4.24	1.26	0.33	5.08
554	14.72	32.51	2419	2234	5.66	1.46	0.36	5.33
555	14.66	32.51	2428	2256	8.18	1.77	0.43	6.04
556	14.68	32.51	2433	2271	9.79	1.87	0.47	6.27
557	14.70	32.50	2438	2273	11.22	2.17	0.50	6.22

Sample No.	DIN [µmol L^{-1}]	C / C_{org} (SPM) [µmol L^{-1}]	N (SPM) [µmol L^{-1}]	C_{org}:N (SPM)	SPM [mg L^{-1}]	Ca / Ar [Ω]	pH	PO_4^{3-} [µmol L^{-1}]
545	4.93	86.8 / 65.1	8.8	7.4	12.8	3.8 / 2.4	8.07	0.12
546	4.83	72.7 / 42.4	7.4	5.8	8.7	3.5 / 2.3	8.03	0.11
547	4.76	112.4 / 93.4	9.6	9.7	15.4	3.7 / 2.3	8.05	0.11
548	4.91	108.5 / 104.6	9.9	10.5	16.8	3.7 / 2.4	8.05	0.12
549	4.73	111.1 / 97.8	8.8	11.1	13.9	3.6 / 2.3	8.01	0.32
550	5.37	233.0 / 180.3	17.7	10.2	32.2	3.3 / 2.1	7.97	0.42
551	5.56	193.2 / 174.3	14.5	12.0	29.6	3.5 / 2.2	7.99	0.47
552	7.08	248.6 / 163.5	18.4	8.9	34.3	3.3 / 2.1	7.96	0.57
553	6.67	257.6 / 199.3	18.3	10.9	41.6	3.2 / 2.1	7.95	0.54
554	7.15	324.4 / 271.1	23.2	11.7	55.0	3.4 / 2.2	7.98	0.54

555	8.24	440.4 / 345.2	29.2	11.8	75.7	3.2 / 2.1	7.95	0.58
556	8.61	430.5 / 363.3	27.9	13.0	82.4	3.1/ 2.0	7.93.	0.62
557	8.90	308.9 / 199.1	21.2	9.4	48.8	3.1 / 2.0	7.93	0.63

Data availability

The data of this study are either presented in the article or are available upon request from the corresponding author.

Author Contributions

MN wrote the manuscript, did the carbon sampling and sample measurement, analyzed and evaluated the data, and led the study. JvB led the research cruise. JvB and HT contributed with editorial and scientific recommendations. MN prepared the manuscript with contribution from all co-authors.

Competing interests

The contact author has declared that none of the authors has any competing interests.

Acknowledgement

We thank the crew from RV *Ludwig Prandtl* for their support during the cruise. We thank Leon Schmidt for the nutrient sampling and measurements, and Marc Metzke for the C/N measurements. We further thank Xinping Hu and two anonymous reviewers for their constructive comments, which greatly improved this manuscript.

Financial support

This research has been funded by the German Academic Exchange Service (DAAD, project: MOPGA-GRI, grant no. 57429828), which received funds from the German Federal Ministry of Education and Research (BMBF).

References

Abril, G., and Frankignoulle, M.: Nitrogen–alkalinity interactions in the highly polluted Scheldt basin (Belgium), Water Research, 35, 844-850, https://doi.org/10.1016/S0043-1354(00)00310-9, 2001.

Beck, M., Dellwig, O., Holstein, J. M., Grunwald, M., Liebezeit, G., Schnetger, B., and Brumsack, H.-J.: Sulphate, dissolved organic carbon, nutrients and terminal metabolic products in deep pore waters of an intertidal flat, Biogeochemistry, 89, 221-238, https://doi.org/10.1007/s10533-008-9215-6, 2008a.

Beck, M., Dellwig, O., Liebezeit, G., Schnetger, B., and Brumsack, H.-J.: Spatial and seasonal variations of sulphate, dissolved organic carbon, and nutrients in deep pore waters of intertidal flat sediments, Estuarine, Coastal and Shelf Science, 79, 307-316, https://doi.org/10.1016/j.ecss.2008.04.007, 2008b.
Berner, R. A., Scott, M. R., and Thomlinson, C.: Carbonate alkalinity in the pore waters of anoxic marine sediments 1, Limnology and Oceanography, 15, 544-549, https://doi.org/10.4319/lo.1970.15.4.0544, 1970.
Berner, R. A., Lasaga, A. C., and Garrels, R. M.: Carbonate-silicate geochemical cycle and its effect on atmospheric carbon dioxide over the past 100 million years, Am. J. Sci.;(United States), 283, doi:10.2475/ajs.283.7.641., 1983.
Billerbeck, M., Werner, U., Polerecky, L., Walpersdorf, E., DeBeer, D., and Huettel, M.: Surficial and deep pore water circulation governs spatial and temporal scales of nutrient recycling in intertidal sand flat sediment, Marine Ecology Progress Series, 326, 61-76, 2006.
Blackburn, T., and Henriksen, K.: Nitrogen cycling in different types of sediments from Danish waters 1, Limnology and Oceanography, 28, 477-493, https://doi.org/10.4319/lo.1983.28.3.0477, 1983.
Borges, A. V., Delille, B., and Frankignoulle, M.: Budgeting sinks and sources of CO_2 in the coastal ocean: Diversity of ecosystems counts, Geophysical research letters, 32, doi.org/10.1029/2005GL023053, 2005.
Bozec, Y., Thomas, H., Elkalay, K., and de Baar, H. J.: The continental shelf pump for CO_2 in the North Sea—evidence from summer observation, Marine Chemistry, 93, 131-147, https://doi.org/10.1016/j.marchem.2004.07.006, 2005.
Brasse, S., Reimer, A., Seifert, R., and Michaelis, W.: The influence of intertidal mudflats on the dissolved inorganic carbon and total alkalinity distribution in the German Bight, southeastern North Sea, Journal of Sea Research, 42, 93-103, 1999.
Brenner, H., Braeckman, U., Le Guitton, M., and Meysman, F. J.: The impact of sedimentary alkalinity release on the water column CO_2 system in the North Sea, Biogeosciences, 13, 841-863, https://doi.org/10.5194/bg-13-841-2016, 2016.
Brewer, P. G., and Goldman, J. C.: Alkalinity changes generated by phytoplankton growth, Limnology and Oceanography, 21, 108-117, https://doi.org/10.4319/lo.1976.21.1.0108, 1976.
Brzezinski, M. A.: The Si: C: N ratio of marine diatoms: interspecific variability and the effect of some environmental variables, Journal of Phycology, 21, 347-357, https://doi.org/10.1111/j.0022-3646.1985.00347.x, 1985.
Burchard, H., Flöser, G., Staneva, J. V., Badewien, T. H., and Riethmüller, R.: Impact of density gradients on net sediment transport into the Wadden Sea, Journal of Physical Oceanography, 38, 566-587, 2008.
Burt, W., Thomas, H., Hagens, M., Pätsch, J., Clargo, N., Salt, L., Winde, V., and Böttcher, M.: Carbon sources in the North Sea evaluated by means of radium and stable carbon isotope tracers, Limnology and Oceanography, 61, 666-683, https://doi.org/10.1002/lno.10243, 2016.
Carter, B. R., Toggweiler, J., Key, R. M., and Sarmiento, J. L.: Processes determining the marine alkalinity and calcium carbonate saturation state distributions, Biogeosciences, 11, 7349-7362, https://doi.org/10.5194/bg-11-7349-2014, 2014.
Charalampopoulou, A., Poulton, A. J., Tyrrell, T., and Lucas, M. I.: Irradiance and pH affect coccolithophore community composition on a transect between the North Sea and the Arctic Ocean, Marine Ecology Progress Series, 431, 25-43, https://doi.org/10.3354/meps09140, 2011.
Chen, C. T. A., and Wang, S. L.: Carbon, alkalinity and nutrient budgets on the East China Sea continental shelf, Journal of Geophysical Research: Oceans, 104, 20675-20686, https://doi.org/10.1029/1999JC900055, 1999.
Crutzen, P.: Geology of mankind, Nature, 415, https://doi.org/10.1038/415023a, 2002.
De Beer, D., Wenzhöfer, F., Ferdelman, T. G., Boehme, S. E., Huettel, M., van Beusekom, J. E., Böttcher, M. E., Musat, N., and Dubilier, N.: Transport and mineralization rates in North Sea sandy intertidal sediments, Sylt-Rømø basin, Wadden Sea, Limnology and Oceanography, 50, 113-127, 2005.
De Jonge, V., Essink, K., and Boddeke, R.: The Dutch Wadden Sea: a changed ecosystem, Hydrobiologia, 265, 45-71, https://doi.org/10.1007/BF00007262, 1993.
Dickson, A., and Millero, F. J.: A comparison of the equilibrium constants for the dissociation of carbonic acid in seawater media, Deep Sea Research Part A. Oceanographic Research Papers, 34, 1733-1743, https://doi.org/10.1016/0198-0149(87)90021-5, 1987.
Dickson, A. G.: An exact definition of total alkalinity and a procedure for the estimation of alkalinity and total inorganic carbon from titration data, Deep Sea Research Part A. Oceanographic Research Papers, 28, 609-623, https://doi.org/10.1016/0198-0149(81)90121-7, 1981.
Elias, E. P., Van der Spek, A. J., Wang, Z. B., and De Ronde, J.: Morphodynamic development and sediment budget of the Dutch Wadden Sea over the last century, Netherlands Journal of Geosciences, 91, 293-310, https://doi.org/10.1017/S0016774600000457, 2012.
Faber, P. A., Evrard, V., Woodland, R. J., Cartwright, I. C., and Cook, P. L.: Pore-water exchange driven by tidal pumping causes alkalinity export in two intertidal inlets, Limnology and Oceanography, 59, 1749-1763, https://doi.org/10.4319/lo.2014.59.5.1749, 2014.
Glavovic, B., Limburg, K., Liu, K., Emeis, K., Thomas, H., Kremer, H., Avril, B., Zhang, J., Mulholland, M., and Glaser, M.: Living on the Margin in the Anthropocene: engagement arenas for sustainability research and action at the ocean–land interface, Current Opinion in Environmental Sustainability, 14, 232-238, https://doi.org/10.1016/j.cosust.2015.06.003, 2015.
Grasshoff, K., Kremling, K., and Ehrhardt, M.: Methods of seawater analysis, John Wiley & Sons, 2009.
Gruber, N., Clement, D., Carter, B. R., Feely, R. A., Van Heuven, S., Hoppema, M., Ishii, M., Key, R. M., Kozyr, A., and Lauvset, S. K.: The oceanic sink for anthropogenic CO_2 from 1994 to 2007, Science, 363, 1193-1199, DOI: 10.1126/science.aau5153, 2019.
Hansen, H., and Koroleff, F.: Determination of nutrients. Methods of Seawater Analysis: Third, Completely Revised and Extended Edition. Grasshoff, K., Kremling, K., and Ehrhardt, M. (Eds.), Weinheim, Germany: Wiley-VCH Verlag GmbH, 2007.

Hoppema, J.: The distribution and seasonal variation of alkalinity in the southern bight of the North Sea and in the western Wadden Sea, Netherlands journal of sea research, 26, 11-23, https://doi.org/10.1016/0077-7579(90)90053-J, 1990.
Hoppema, J.: The oxygen budget of the western Wadden Sea, The Netherlands, Estuarine, Coastal and Shelf Science, 32, 483-502, https://doi.org/10.1016/0272-7714(91)90036-B, 1991.
Hoppema, J.: Carbon dioxide and oxygen disequilibrium in a tidal basin (Dutch Wadden Sea), Netherlands journal of sea research, 31, 221-229, https://doi.org/10.1016/0077-7579(93)90023-L, 1993.
Hu, X., and Cai, W. J.: An assessment of ocean margin anaerobic processes on oceanic alkalinity budget, Global Biogeochemical Cycles, 25, doi.org/10.1029/2010GB003859, 2011.
Jahnke, R. A., Craven, D. B., and Gaillard, J.-F.: The influence of organic matter diagenesis on $CaCO_3$ dissolution at the deep-sea floor, Geochimica et Cosmochimica Acta, 58, 2799-2809, 1994.
Jensen, K., Jensen, M., and Kristensen, E.: Nitrification and denitrification in Wadden Sea sediments (Königshafen, Island of Sylt, Germany) as measured by nitrogen isotope pairing and isotope dilution, Aquatic Microbial Ecology, 11, 181-191, doi:10.3354/ame011181, 1996.
Keith, D. W., Ha-Duong, M., and Stolaroff, J. K.: Climate strategy with CO_2 capture from the air, Climatic Change, 74, 17-45, https://doi.org/10.1007/s10584-005-9026-x, 2006.
Kérouel, R., and Aminot, A.: Fluorometric determination of ammonia in sea and estuarine waters by direct segmented flow analysis, Marine Chemistry, 57, 265-275, https://doi.org/10.1016/S0304-4203(97)00040-6, 1997.
Kieskamp, W. M., Lohse, L., Epping, E., and Helder, W.: Seasonal variation in denitrification rates and nitrous oxide fluxes in intertidal sediments of the western Wadden Sea, Marine ecology progress series. Oldendorf, 72, 145-151, 1991.
Lewis, E., and Wallace, D.: Program developed for CO_2 system calculations, Environmental System Science Data Infrastructure for a Virtual Ecosystem, 1998.
Louters, T., and Gerritsen, F.: The Riddle of the Sands: A Tidal SystenVs Answer to a Rising Sea Level, report RIKZ-94.040 (isbn 90-369-0084-0), 1994.
Luff, R., and Moll, A.: Seasonal dynamics of the North Sea sediments using a three-dimensional coupled sediment–water model system, Continental Shelf Research, 24, 1099-1127, https://doi.org/10.1016/j.csr.2004.03.010, 2004.
Martin, W., and Sayles, F.: $CaCO_3$ dissolution in sediments of the Ceara Rise, western equatorial Atlantic, Geochimica et Cosmochimica Acta, 60, 243-263, https://doi.org/10.1016/0016-7037(95)00383-5, 1996.
Matthews, H. D., and Caldeira, K.: Stabilizing climate requires near-zero emissions, Geophysical research letters, 35, https://doi.org/10.1029/2007GL032388, 2008.
Mehrbach, C., Culberson, C., Hawley, J., and Pytkowicx, R.: Measurement of the apparent dissociation constants of carbonic acid in seawater at atmospheric pressure, Limnology and oceanography, 18, 897-907, https://doi.org/10.4319/lo.1973.18.6.0897, 1973.
Meister, P., Herda, G., Petrishcheva, E., Gier, S., Dickens, G. R., Bauer, C., and Liu, B.: Microbial Alkalinity Production and Silicate Alteration in Methane Charged Marine Sediments: Implications for Porewater Chemistry and Diagenetic Carbonate Formation, Geochemical Signals in Dynamic Sedimentary Systems Along Continental Margins, 2022.
Meybeck, M.: Global chemical weathering of surficial rocks estimated from river dissolved loads, American journal of science, 287, 401-428, 10.2475/ajs.287.5.401, 1987.
Middelburg, J. J., Soetaert, K., and Hagens, M.: Ocean alkalinity, buffering and biogeochemical processes, Reviews of Geophysics, 58, e2019RG000681, https://doi.org/10.1029/2019RG000681, 2020.
Norbisrath, M., Pätsch, J., Dähnke, K., Sanders, T., Schulz, G., van Beusekom, J. E., and Thomas, H.: Metabolic alkalinity release from large port facilities (Hamburg, Germany) and impact on coastal carbon storage, Biogeosciences, 19, 5151-5165, https://doi.org/10.5194/bg-19-5151-2022, 2022.
Norbisrath, M., Neumann, A., Dähnke, K., Sanders, T., Schöl, A., van Beusekom, J. E., and Thomas, H.: Alkalinity and nitrate dynamics reveal dominance of anammox in a hyper-turbid estuary, Biogeosciences, 20, 4307–4321, https://doi.org/10.5194/bg-20-4307-2023, 2023.
Petersen, W., Schroeder, F., and Bockelmann, F.-D.: FerryBox-Application of continuous water quality observations along transects in the North Sea, Ocean Dynamics, 61, 1541-1554, https://doi.org/10.1007/s10236-011-0445-0, 2011.
Postma, H.: Hydrography of the Dutch Wadden sea, Arch. Neerl. Zool, 10, 405-511, 1954.
Renforth, P., and Henderson, G.: Assessing ocean alkalinity for carbon sequestration, Reviews of Geophysics, 55, 636-674, https://doi.org/10.1002/2016RG000533, 2017.
Ridderinkhof, H., Zimmerman, J., and Philippart, M.: Tidal exchange between the North Sea and Dutch Wadden Sea and mixing time scales of the tidal basins, Netherlands Journal of Sea Research, 25, 331-350, https://doi.org/10.1016/0077-7579(90)90042-F, 1990.
Røy, H., Lee, J. S., Jansen, S., and de Beer, D.: Tide-driven deep pore-water flow in intertidal sand flats, Limnology and oceanography, 53, 1521-1530, https://doi.org/10.4319/lo.2008.53.4.1521, 2008.
Rutgers van der Loeff, M.: Transport van reactief silikaat uit Waddenzee sediment naar het bovenstaande water, NIOZ-rapport, 1974.
Sabine, C. L., Feely, R. A., Gruber, N., Key, R. M., Lee, K., Bullister, J. L., Wanninkhof, R., Wong, C., Wallace, D. W., and Tilbrook, B.: The oceanic sink for anthropogenic CO_2, science, 305, 367-371, DOI: 10.1126/science.1097403, 2004.

Santos, I. R., Chen, X., Lecher, A. L., Sawyer, A. H., Moosdorf, N., Rodellas, V., Tamborski, J., Cho, H.-M., Dimova, N., and Sugimoto, R.: Submarine groundwater discharge impacts on coastal nutrient biogeochemistry, Nature Reviews Earth & Environment, 2, 307-323, https://doi.org/10.1038/s43017-021-00152-0, 2021.
Schwichtenberg, F., Callies, U., and van Beusekom, J. E.: Residence times in shallow waters help explain regional differences in Wadden Sea eutrophication, Geo-Marine Letters, 37, 171-177, https://doi.org/10.1007/s00367-016-0482-2, 2017.
Schwichtenberg, F., Pätsch, J., Böttcher, M. E., Thomas, H., Winde, V., and Emeis, K.-C.: The impact of intertidal areas on the carbonate system of the southern North Sea, Biogeosciences, 17, 4223-4245, https://doi.org/10.5194/bg-17-4223-2020, 2020.
Shadwick, E., Thomas, H., Gratton, Y., Leong, D., Moore, S., Papakyriakou, T., and Prowe, A.: Export of Pacific carbon through the Arctic Archipelago to the North Atlantic, Continental Shelf Research, 31, 806-816, https://doi.org/10.1016/j.csr.2011.01.014, 2011.
Suchet, P. A., and Probst, J.-L.: Modelling of atmospheric CO_2 consumption by chemical weathering of rocks: application to the Garonne, Congo and Amazon basins, Chemical Geology, 107, 205-210, DOI:10.1016/0009-2541(93)90174-H, 1993.
Thomas, H., Bozec, Y., Elkalay, K., and De Baar, H. J.: Enhanced open ocean storage of CO_2 from shelf sea pumping, Science, 304, 1005-1008, DOI: 10.1126/science.1095491, 2004.
Thomas, H., Schiettecatte, L.-S., Suykens, K., Koné, Y., Shadwick, E., Prowe, A. F., Bozec, Y., de Baar, H. J., and Borges, A.: Enhanced ocean carbon storage from anaerobic alkalinity generation in coastal sediments, Biogeosciences, 6, 267-274, https://doi.org/10.5194/bg-6-267-2009, 2009.
Van Bennekom, A., Krijgsman-van Hartingsveld, E., Van der Veer, G., and Van Voorst, H.: The seasonal cycles of reactive silicate and suspended diatoms in the Dutch Wadden Sea, Netherlands Journal of Sea Research, 8, 174-207, https://doi.org/10.1016/0077-7579(74)90016-7, 1974.
Van Beusekom, J., Brockmann, U., Hesse, K.-J., Hickel, W., Poremba, K., and Tillmann, U.: The importance of sediments in the transformation and turnover of nutrients and organic matter in the Wadden Sea and German Bight, Deutsche Hydrografische Zeitschrift, 51, 245-266, 10.1007/BF02764176, 1999.
Van Beusekom, J., and De Jonge, V.: Long-term changes in Wadden Sea nutrient cycles: importance of organic matter import from the North Sea, in: Nutrients and Eutrophication in Estuaries and Coastal Waters, Springer, 185-194, 2002.
Van Beusekom, J. E., Buschbaum, C., and Reise, K.: Wadden Sea tidal basins and the mediating role of the North Sea in ecological processes: scaling up of management?, Ocean & coastal management, 68, 69-78, https://doi.org/10.1016/j.ocecoaman.2012.05.002, 2012.
Van Beusekom, J. E., Carstensen, J., Dolch, T., Grage, A., Hofmeister, R., Lenhart, H., Kerimoglu, O., Kolbe, K., Pätsch, J., and Rick, J.: Wadden Sea Eutrophication: long-term trends and regional differences, Frontiers in Marine Science, 6, 370, doi.org/10.3389/fmars.2019.00370, 2019.
Van Der Zee, C., and Chou, L.: Seasonal cycling of phosphorus in the Southern Bight of the North Sea, Biogeosciences, 2, 27-42, https://doi.org/10.5194/bg-2-27-2005, 2005.
van Raaphorst, W., and van der Veer, H. W.: The phosphorus budget of the Marsdiep tidal basin (Dutch Wadden Sea) in the period 1950–1985: importance of the exchange with the North Sea, in: North Sea—Estuaries Interactions, Springer, 21-38, 1990.
Voynova, Y. G., Petersen, W., Gehrung, M., Aßmann, S., and King, A. L.: Intertidal regions changing coastal alkalinity: The Wadden Sea-North Sea tidally coupled bioreactor, Limnology and Oceanography, 64, 1135-1149, 2019.
Wang, Z. A., Kroeger, K. D., Ganju, N. K., Gonneea, M. E., and Chu, S. N.: Intertidal salt marshes as an important source of inorganic carbon to the coastal ocean, Limnology and Oceanography, 61, 1916-1931, 2016.
Waska, H., and Kim, G.: Submarine groundwater discharge (SGD) as a main nutrient source for benthic and water-column primary production in a large intertidal environment of the Yellow Sea, Journal of Sea Research, 65, 103-113, https://doi.org/10.1016/j.seares.2010.08.001, 2011.
Wolf-Gladrow, D. A., Zeebe, R. E., Klaas, C., Körtzinger, A., and Dickson, A. G.: Total alkalinity: The explicit conservative expression and its application to biogeochemical processes, Marine Chemistry, 106, 287-300, https://doi.org/10.1016/j.marchem.2007.01.006, 2007.
Wu, Z., Zhou, H., Zhang, S., and Liu, Y.: Using ^{222}Rn to estimate submarine groundwater discharge (SGD) and the associated nutrient fluxes into Xiangshan Bay, East China Sea, Marine pollution bulletin, 73, 183-191, https://doi.org/10.1016/j.marpolbul.2013.05.024, 2013.
Zalasiewicz, J., Williams, M., Steffen, W., and Crutzen, P.: The new world of the Anthropocene. ACS Publications, 2010.
Zhang, C., Shi, T., Liu, J., He, Z., Thomas, H., Dong, H., Rinkevich, B., Wang, Y., Hyun, J.-H., and Weinbauer, M.: Eco-engineering approaches for ocean negative carbon emission, Science Bulletin, 67, 2564-2573, https://doi.org/10.1016/j.scib.2022.11.016, 2022.